

## Planck on the knowledge of the microwave sky, a milestone for the road to future experiments

---

**Daniela Paoletti\*** *on behalf of the Planck Collaboration*

*Osservatorio di Astrofisica e Scienza dello Spazio di Bologna/Istituto Nazionale di Astrofisica,  
via Gobetti 101, I-40129 Bologna, Italy*

*Istituto Nazionale Di Fisica Nucleare, Sezione di Bologna, Viale Berti Pichat, 6/2, I-40127  
Bologna, Italy*

*E-mail: [paoletti@iasfbo.inaf.it](mailto:paoletti@iasfbo.inaf.it)*

The Planck satellite dedicated to the observation of the Cosmic Microwave Background (CMB), has observed the microwave sky providing full sky maps at nine frequencies between 30 GHz and 857 GHz with unprecedented precision. Planck observations allowed to perform the most accurate analysis of the different emissions which compose the microwave sky providing descriptions of the phenomena involved which will be the legacy for years to come. I will describe how Planck data allowed to perform an accurate component separation which provides the most precise CMB full sky maps in temperature and polarization together with maps and descriptions of the single foreground components, from the lowest to the highest frequency channels. I will describe also the power spectrum approach which is used in the derivation of the cosmological parameters and how it accounts for foreground residuals and secondary anisotropies. Finally I will conclude with a look to the future of CMB observations and how the Planck legacy will be the starting point for the future experiments.

*Frontier Research in Astrophysics - III (FRAPWS2018)*

*28 May - 2 June 2018*

*Mondello (Palermo), Italy*

---

\*Speaker.

## 1. Introduction

The Cosmic Microwave Background radiation (CMB) is the thermal relic from the Hot Big Bang. It was emitted at around  $z \sim 1080$  when the universe temperature was cool enough to allow the hydrogen recombination, neutralizing the universe which became optically thin. CMB photons have been redshifted by the universe expansion to the microwave band and follow an almost perfect black body spectrum with a peak at  $\lambda \sim 1$  cm. The black body has an absolute temperature of  $T_0 = 2.72548 \pm 0.00057K$  [1] which was measured by the FIRAS instrument onboard the COBE satellite, the first generation of CMB dedicated space experiments<sup>1</sup>. The CMB is isotropic on the sky but for small anisotropies of the order of  $\Delta T/T \sim 10^{-5}$ . These anisotropies are the footprints of primordial perturbations in the matter which are the seeds that through gravitational instability have formed the large scale structures we observe today such as galaxies and galaxy clusters. The CMB represents the most important observational window open on the early Universe and its observation is crucial for the understanding of the cosmological model which describes our Universe. CMB observations, either on small angular scales from the ground based and balloon born experiments, or on the whole sky from space satellites, are both technologically and scientifically challenging. In fact, the microwave sky is composed not only by the CMB but by a superposition of different signals among which the CMB is dominant only for a very narrow frequency range centered in 70-90 GHz. In Fig.1 we show the CMB map as derived in Planck 2015 results (left panel) compared with the CMB subtracted map (right panel) which evidences the strong contamination of the microwave sky by astrophysical signals. In this work we will describe the current status of the microwave observations, the two approach to CMB data: on one side the map approach which cleans the data through the component separation algorithm and produce CMB cleaned maps used for scientific results on large angular scales and on the other side the power spectrum approach used to derive cosmological parameters with the addition of data on small angular scales.

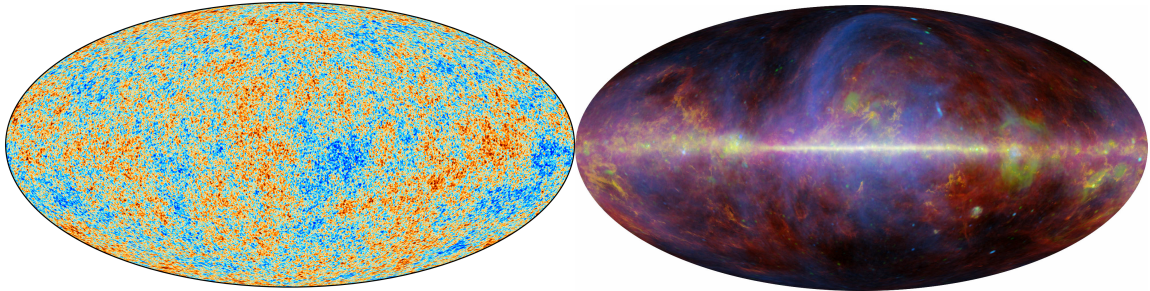


**Figure 1:** On the left panel we show the CMB SMICA map of Planck 2015. On the right the microwave sky with the CMB subtracted.

## 2. Planck

Planck is a mission of the European space agency and represents the third generation of satellites dedicated to the observation of the microwave sky after the NASA satellites COBE and WMAP. Planck was born in 1998 by the merger of two proposal, COBRAS and SAMBA. It was

<sup>1</sup><https://lambda.gsfc.nasa.gov/product/cobe/>

launched in May 2009 and has acquired data until October 2013. Planck was orbiting around the Lagrangian point L2 performing a full sky survey every six months, with a resolution up to 5' and a sensitivity up to  $2\mu\text{K}$  [2]. The satellite has two instruments on board: the Low Frequency Instrument LFI composed by HEMT receivers at 30, 44 and 70 GHz and the High Frequency Instrument HFI composed by spiderweb bolometers at 100, 143, 217, 353, 545, 857 GHz. The frequency channels from 30 up to 353 GHz were also polarization sensitive. The first data release, only temperature data from the nominal mission, took place in March 2013 [3]; in February 2015 took place the second data release based on full mission data in temperature and polarization, with the exclusion of the large angular scale polarization coming from the HFI instrument which was still contaminated by systematics [2]. The results I will present in the following are part of the 2015 release. After this talk was completed on the 17<sup>th</sup> of July 2018 the final legacy release of Planck with the full temperature and polarization data was delivered to the public [4].

The microwave sky is the composition of CMB, several astrophysical emissions and secondary anisotropies. Astrophysical emissions span from the lowest to the highest frequencies and have different origins and spectral shapes. The main ones are synchrotron, dust emission (thermal and spinning), free-free and CO lines. Secondary anisotropies are CMB anisotropies generated after recombination, due to their later generation with respect to primary anisotropies which are connected to the primordial universe, encode the travel of the photons from the last scattering surface to the observer. The main secondary anisotropies are: the lensing deflection of CMB photons by the large scale structure, the integrated Sachs Wolfe effect which accounts for the net red- or blue- shift of the photons travelling through a time varying gravitational potential and finally the Sunyaev Zeldovich effect. The Integrated Sachs-Wolfe effect is not separable from primary anisotropies and therefore remains included in the primary CMB signal in the data and is considered in the theoretical predictions in the likelihood.

### 3. The map approach

In order to derive the full-sky CMB map of Fig.1 from the data it is necessary to perform what is called *component separation*, a process which disentangles the different components of the sky separating each signal from the others and produces cleaned CMB maps.

#### 3.1 The microwave sky seen by Planck

Planck has not only provided cosmological results but has also changed the paradigm of the microwave sky. In Fig.2 we show the comparison of the different astrophysical emission spectral shapes as they were known before Planck on the left and how are known now after Planck on the right. We note how the relative importance of free-free and synchrotron has been inverted and we note also how Planck observations allowed to characterize the spinning dust emission previously known only as an anomalous microwave emission. Component separation algorithms use the different frequency dependences of the various emissions to distinguish and separate one from the others. The use of the spectral shape implies that in order to perform a good component separation a CMB experiment requires a wide frequency range and a very high number of frequencies, the more the better. In this sense, Planck with its nine frequency channels spanning from 30 GHz to

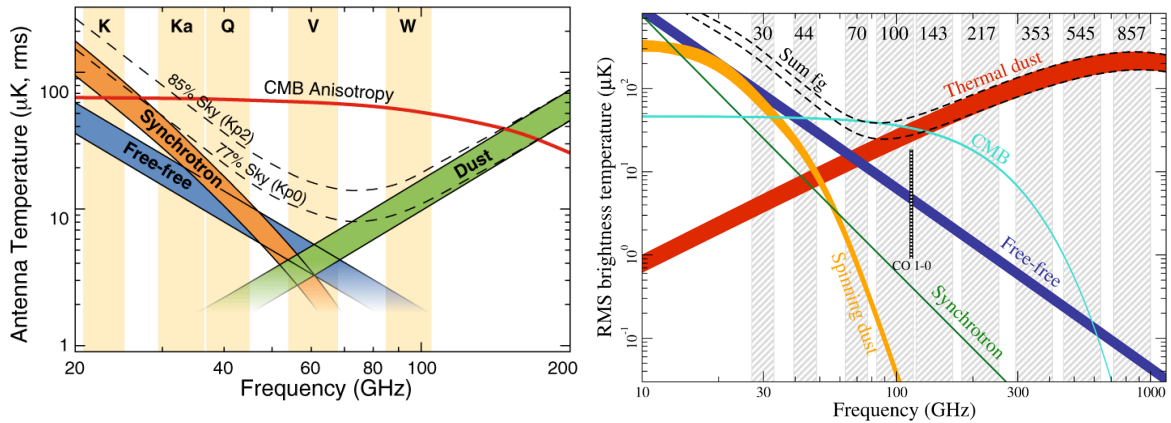


**Figure 2:** On the left panel we show microwave emissions as seen by WMAP. On the right the microwave emissions as seen by Planck.

1THz represents the best current experiment for component separation. Planck uses four different algorithms for component separation which are based on different methods.

- Smica: Spectral Matching Independent Component Analysis in wavelet space;
- Nilc: Internal linear combination in needled space;
- Sevem: Template fitting approach that provides also cleaned single frequency CMB maps ;
- Commander: Bayesian analysis parameter fitting method, together with the CMB it provides single component maps and fits for the parameters of the emissions.

Since we are interested both in the CMB and astrophysical emissions we will focus on the Commander results which provide an accurate characterization of all the components. We remark that all the four component separation algorithms provide results in perfect agreement with each other. The Commander algorithm [5, 6] models the different components through spectral templates and fits for parameters describing the involved emissions. It considers not only spatially uniform global parameters but also different parameters for each pixel in order to maximize the freedom: it fits for 11 million parameters for low resolution and 200 million parameters for high resolution maps. Commander uses a multiresolution approach which derives the CMB map up to the maximum resolution of the satellite of  $5'$  whereas the astrophysical emissions like thermal dust and CO are at  $7'.5$  resolution whilst synchrotron, spinning dust and free-free emission are at  $1^\circ$  resolution. The analysis involves all the nine Planck channels 30-857 GHz but includes also WMAP 9 year K, Ka, Q, V and W bands [7] in addition is included also the Haslam destriped map at 408 MHz [8] to better cover the lowest frequencies. We will describe the details of the Commander results on the single components of the microwave sky in the following.

### 3.1.1 CMB

The reconstructed full resolution CMB temperature map from Commander is shown in Fig.3 [9]. We note the very good agreement with Fig.1 which was derived with the SMICA component

separation algorithm. The differences in the region of the galactic plane is simply due to the fact that SMICA applies the inpainting technique whereas commander does not. However we note that this region is within the common mask which is applied for the cosmological analyses and therefore does not impact the results. As mentioned the different component separation algorithms are all in agreement. The CMB is linearly polarized, the Compton scattering between photons

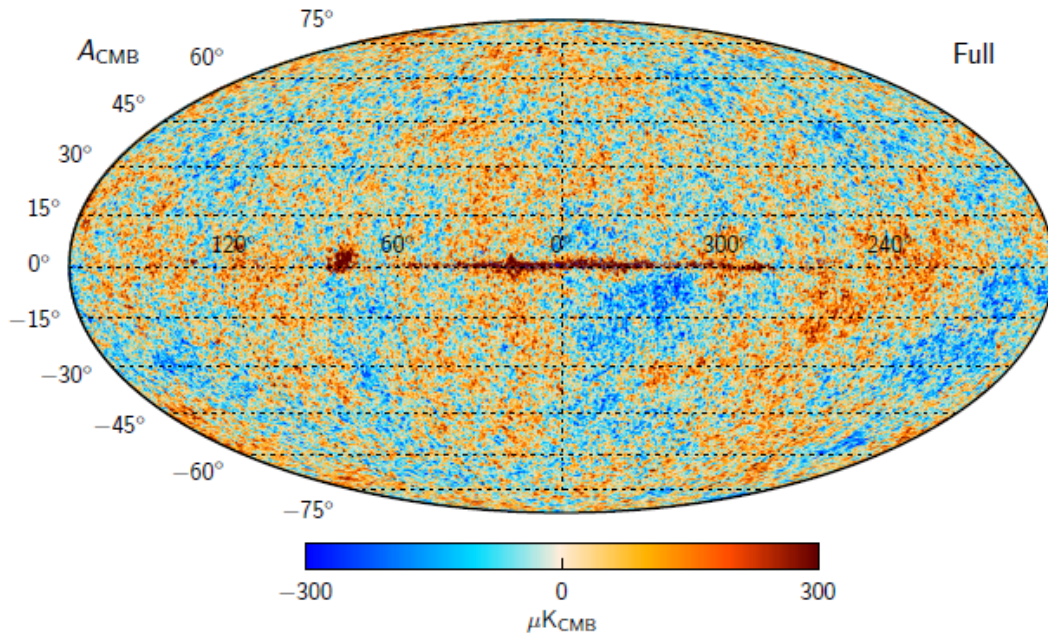


**Figure 3:** CMB temperature map reconstructed from Commander algorithm.

and electrons on a photon distribution with a quadrupolar anisotropy induces a linear polarization. Planck with its seven polarized frequency channels was able to provide the best measurement of CMB full sky polarization to date. In Fig.4 we show the two Stokes parameter maps [9]. A high precision measurement of the CMB polarization anisotropies is the biggest challenge for future CMB experiments.

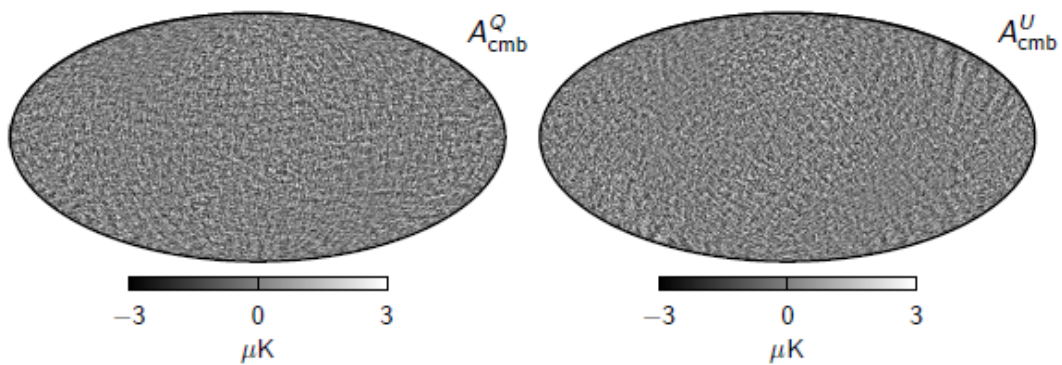


**Figure 4:** CMB Q and U maps reconstructed from Commander algorithm [9].

The CMB polarization is not analysed in terms of Q and U Stokes parameters due to their dependence on the reference system, the combinations of Q and U called E and B which are respectively the gradient and curl-like components of CMB polarization are generally used for the cosmological analysis. E and B signals have different patterns and a different nature due to their parity properties. The E-mode polarization is generated by all kind of cosmological perturbations whereas primary B-mode polarization is produced only by primordial gravitational waves, or other exotic mechanisms like primordial magnetic fields and cosmological birefringence; also the CMB lensing which rotates the E mode generates a secondary B-mode. The even cross-correlation between temperature and E-mode is very useful in adding information whereas odd correlators T-B and E-B are zero in absence of parity violating processes.

### 3.2 The microwave foregrounds

We now describe the major characteristic of the astrophysical signals reconstructed by Planck. In Fig.5 we show the models of the spectra which have been used for the different signals in the analysis.

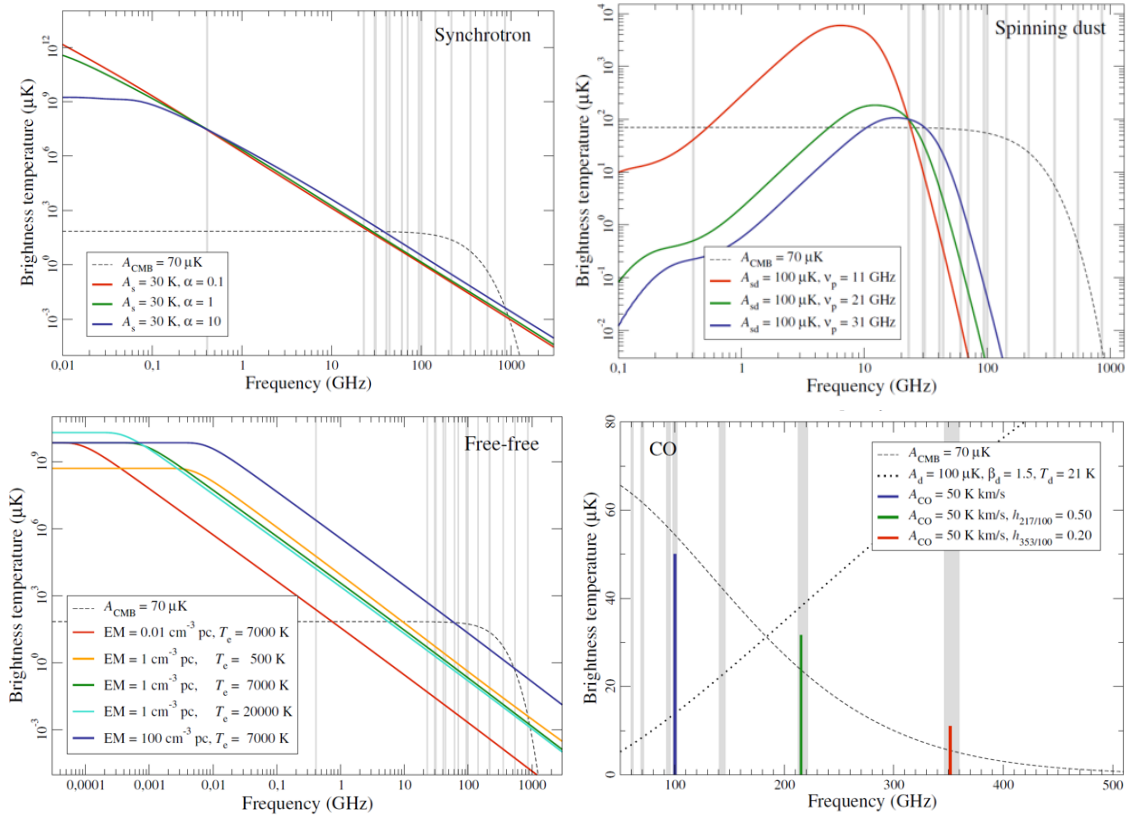


**Figure 5:** Different energy spectra for the four main large scale emissions. Upper left is the synchrotron, upper right is the spinning dust, lower left is the free-free and lower right are the CO lines [10].

#### 3.2.1 Synchrotron

The synchrotron radiation is produced by the free electrons spiralling into the Galactic mag-

netic field. It is intrinsically highly polarized with a 30-40% amplitude in polarization at high galactic latitudes. It represents the dominant contamination contribution for polarization measurements at low and intermediate frequencies with a minor contribution up to 100 and 143 GHz which makes the synchrotron relevant also in the higher frequency channels which therefore need to be cleaned from this contribution as well. It is modelled with a power law:  $s_s = A_s \left(\frac{\nu_0}{\nu}\right)^2 \frac{f_s(\frac{\nu}{\alpha})}{f_s(\frac{\nu_0}{\alpha})}$  with  $\nu_0 = 408\text{ MHz}$  and  $f_s(\nu)$  is an external template from GALPROP<sup>2</sup>. The power law model is well representative down to frequencies as low as 20 GHz, for lower frequencies the spectrum flattens. The spectral behaviour of the model is shown in the upper left panel of Fig.5 for different parameters [10].

Using this model the Commander algorithm fitted for the synchrotron parameters and provided a full sky reconstruction. In Fig.6 we show the reconstructed maps for the synchrotron amplitude in temperature and polarization. The temperature map is rescaled to 408 MHz (i.e. the frequency of the Haslam map) whereas in polarization is rescaled to 30 GHz the lowest Planck channel which is used as a tracer for the synchrotron [10].

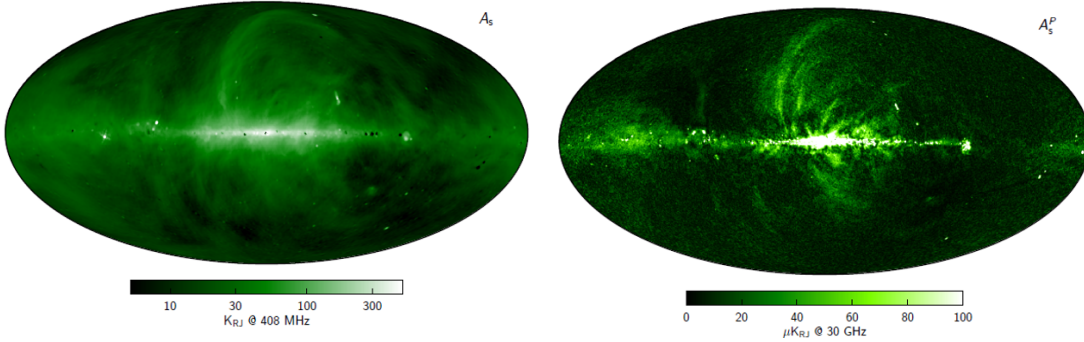


**Figure 6:** In the left we show the reconstructed amplitude map in temperature at 408 MHz. In the right the amplitude in polarization at 30 GHz [10].

### 3.2.2 Spinning dust

The spinning dust emission is produced by the rotation of dust grains. If there is an electric dipole associated to the grain the rotation generates an emission which is in the microwave band. Before its description as spinning dust done with Planck data, the spinning dust emission was detected by WMAP and called Anomalous Microwave Emission (AME). It is described as a two components model characterized by a knee frequency. The two components assume different behaviours of the knee frequency, in one component, labelled as 1, it is considered as a free parameter in each pixel whereas in the other component, labelled as 2, it is considered spatially constant. The model is  $s_{sd} = A_{sd} \cdot \left(\frac{\nu_0}{\nu}\right)^2 \frac{f_{sd}(\nu \cdot \nu_{p0}/\nu_p)}{f_{sd}(\nu_0 \cdot \nu_{p0}/\nu_p)}$  with  $A_{sd}^1, A_{sd}^2 > 0$ ,  $\nu_p^1 \sim N(19 \pm 3\text{ GHz})$ ,  $\nu_p^2 > 0$ , spatially constant,  $\nu_0^1 = 22.8\text{ GHz}$ ,  $\nu_0^2 = 41.0\text{ GHz}$ ,  $\nu_{p0} = 30.0\text{ GHz}$  and finally  $f_{sd}(\nu)$  is given by an external template. It is shown in the upper right panel of Fig.5 [10]. The spinning dust model is fitted within Commander and in Fig.7 we show the two reconstructed maps. On the left panel there is the map of the amplitude rescaled at 30 GHz, whereas on the right there is the reconstructed map of the knee frequency of the variable component [10]. The spinning dust is very

<sup>2</sup><https://galprop.stanford.edu/>

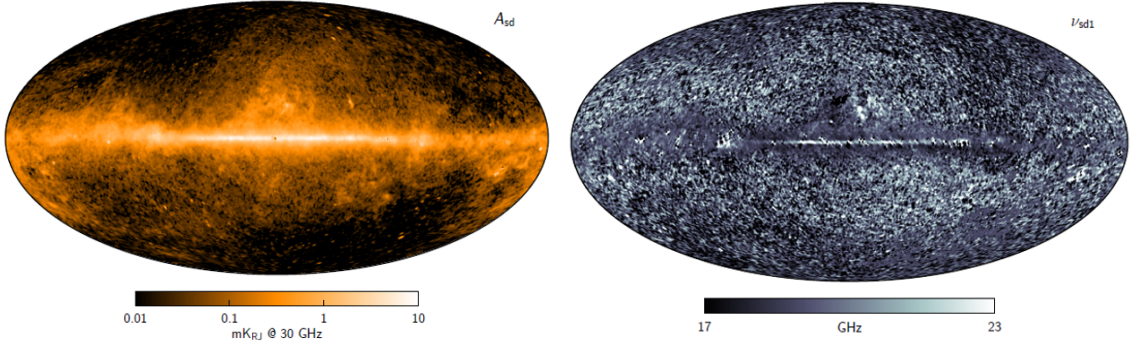


**Figure 7:** On the left panel we show the spinning dust amplitude map. In the right the knee frequency map of component 1 [10].

weakly polarized,  $< 1\%$  and therefore it is not accounted for in polarization analysis.

### 3.2.3 Free-free

The free-free emission is the Bremsstrahlung radiation from the free electrons in our Galaxy. It is usually modelled as a power law for frequencies higher than 1 GHz. It is characterized by the emission measure (the integrated squared electron density), which determines the amplitude of the emission, and by the electron temperature which changes slightly the spectral index. It extends up to the higher frequency channels of Planck. The free-free emission model is  $s_{\text{ff}} = 10^6 T_e (1 - e^{-\tau})$  with  $\tau = 0.05468 * T_e^{-3/2} * \nu_9^{-2} * EM * g_{\text{ff}}$  with  $g_{\text{ff}} = \log \left\{ \exp \left[ 5.960 - \sqrt{3} / \pi \log(\nu_9 * T_4^{-3/2}) \right] + e \right\}$ ,  $T_4 = T_e / 10^4$ ,  $\nu_9 = \nu / (10^9 \text{ Hz})$ ,  $\log EM \sim \text{Uni}(-\infty, \infty)$  and  $T_e \sim N(7000 \pm 500 \text{ K})$ . The frequency spectrum is shown for different choices of parameters in the lower left panel of Fig.5 [10]. The model is fitted and the resulting amplitude map is shown in Fig.8. The polarization is on average very low and therefore it is negligible at microwave frequencies [10].

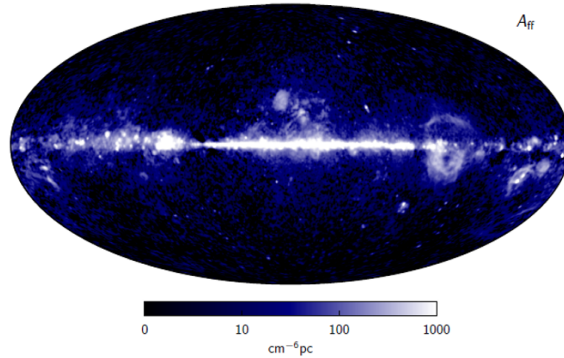


**Figure 8:** Free-free reconstructed amplitude map [10].

### 3.2.4 Degeneracies

The three signals: synchrotron, spinning dust and free-free are correlated and show a degeneracy which means that we can realize the same observed signal with different sets of parameters

making it impossible to disentangle one signal from the other. The combination of channels from Planck, WMAP and the Haslam map has allowed for the first time to contemporarily fit for all the three components together but a certain degree of degeneracy still remains. This residual degeneracy may explain some discrepancies which are observed between the results of Planck combined with WMAP and Haslam and the ones from WMAP alone where the latter exhibits an higher synchrotron contribution and a smaller spinning dust amplitude [11]. Very low frequency observations, below 20 GHz, may play a crucial role in breaking this degeneracy in the future.

### 3.2.5 CO emission and other lines

Planck has performed the first full sky map of the carbon monoxide, CO, emission and it considers all the three transitions  $1 \rightarrow 0$ ,  $2 \rightarrow 1$  and  $3 \rightarrow 2$ . CO lines are very bright in the Planck HFI channels at 100, 143 and 217 GHz and their removal represents a challenge for the component separation. Together with the CO lines the main emission line in the Planck frequency range are the HCN line at 88.6 GHz which contaminates at the 23% level in amplitude the 100 GHz channel near the Galactic circumnuclear disk and Srg A, and the CN, HCO, CS which are present at a level of 5-10% each. Planck is capable to separate the lines and remove them using the individual detector maps. In fact, the bandpass filters of the individual detectors have a different responses for the lines therefore using detector difference maps is possible to detect and map them. Even though the lines are detected and removed the CO residual still represents one of the stronger residual systematic after component separation. The residuals enter in the temperature to polarization leakage, which represents the main systematics in polarization measurements. In order to not be contaminated by the CO leakage for polarization studies it is applied a specific CO mask. The emission for each line/transition  $i$  and detector  $j$  is modelled as  $s_i = A_i h_{ij} \frac{F_i(\nu_j) g(\nu_0)}{F_i(\nu_0) g(\nu_j)}$  and shown in the lower right panel in Fig.5 [10]. In Fig.9 we show the three maps for the different CO transitions and the 94/100 lines [10].

### 3.2.6 Thermal dust emission

Thermal dust represents the main contaminant at high frequencies in both temperature and polarization. It extends up to very high Galactic latitudes and completely dominates the frequencies higher than 200 GHz. The knowledge of the dust contamination is crucial for the future CMB observations. One of the main future challenges is the measurements of the B-mode polarization which is often called the smoking gun of inflation since, if of primordial origin, a B-mode signal would be directly related to the tensor to scalar ratio and consequently to the energy scale of inflation. But the thermal dust through the alignment of the dust grains to the magnetic field produces a polarization signal and in particular a B-mode signal at large and intermediate angular scales. This represents the main contamination of B-mode polarization as shown for example by the joint Planck-BICEP re-analysis of the first B-mode detection on a few degrees angular scale [12] which showed how the data were compatible with dust emission.

The characteristics of the dust signal are determined by the dust polarization but also by the grain characteristics. It is modelled with a modified black body, a superposition of black bodies also called grey body, with free emissivity index and temperature per pixel. The spectrum is given by  $s_d = A_d \cdot \left(\frac{\nu}{\nu_0}\right)^{\beta_d+1} \frac{\exp(\gamma\nu_0)-1}{\exp(\gamma\nu)-1}$  with  $A_d > 0$ ,  $\beta_d \sim N(1.55 \pm 0.1)$ ,  $T_d \sim N(23 \pm 3 \text{ K})$ ,  $\gamma = \frac{h}{k_B T_d}$  and

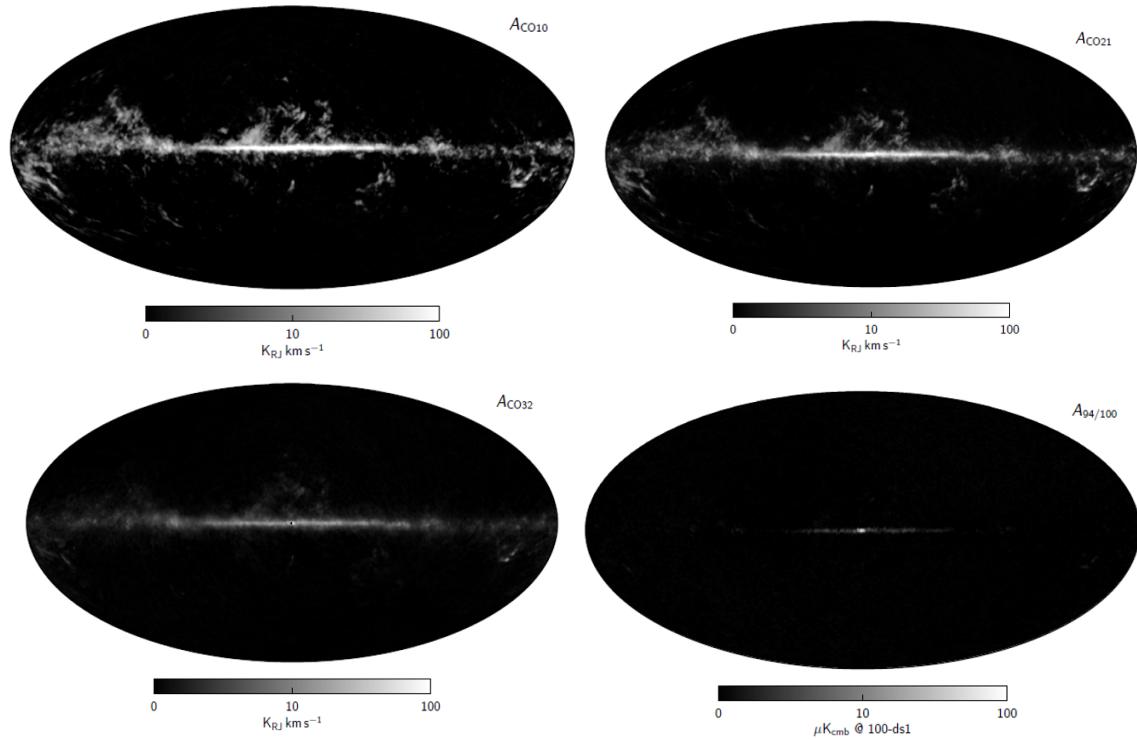


**Figure 9:** CO reconstructed maps. The upper left panel is the  $CO_{1\rightarrow 0}$  line. Upper right is  $CO_{2\rightarrow 1}$ . Lower left and right panel corresponds to  $CO_{3\rightarrow 2}$  and the intensity of the 94/100 lines [10].

$\nu_0 = 545$  GHz [10]. Planck model is accurate up to 857 GHz, beyond this frequency the spectrum assumes a much more complex shape. In the 2015 analysis which is presented here, the thermal dust contribution accounts also for the Cosmic Infrared Background, that is the background formed by the dusty red galaxies, which gives a similar signal to the thermal dust but with a much weaker amplitude. In Fig.10 we present the reconstructed maps of the dust signal amplitude and the spectral index which show the spatial variation and extension of the contamination [10].

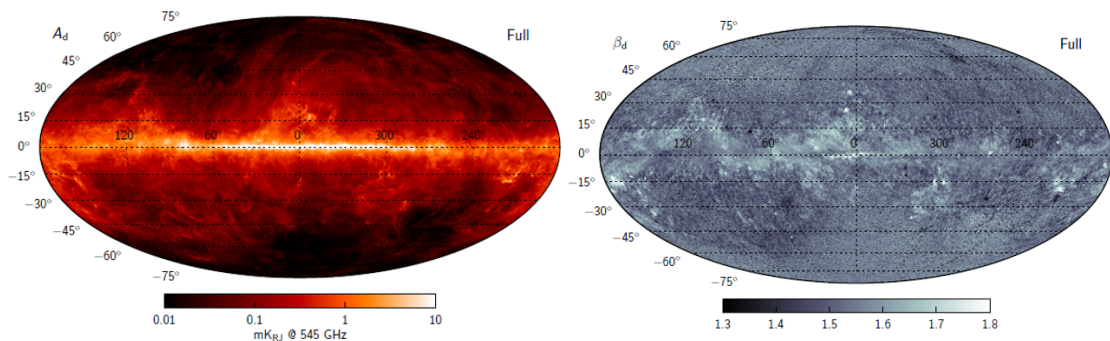


**Figure 10:** On the left panel we show the thermal dust amplitude map. On the right the spectral index map [10].

## 4. The power spectra approach

Using the component separation algorithms it is possible to separate the different diffuse components of the microwave sky and derive a cleaned CMB map. Component separation is optimized for the study of large and intermediate angular scales, the study of cosmological parameters describing the cosmological models requires the addition of high resolution data and therefore high resolution data analysis tools. Component separated maps represent only the large scale part of the Planck likelihood which on small angular scales is based on angular power spectra and in particular on cross-spectra which provide the lowest noise level. On small angular scales the contamination of the diffuse foregrounds is either negligible or under control but the spectra are contaminated by undetected point sources and secondary anisotropy residuals.

### 4.1 The Planck power spectra

The CMB anisotropies are expanded in spherical harmonics:  $\Delta_T(\vec{x}, \hat{n}, \tau) = \sum_{l=1}^{\infty} \sum_{m=-l}^l a_{lm}(\vec{x}, \tau) Y_{lm}(\hat{n})$ . and the angular power spectrum is defined as  $C_l = \frac{1}{2l+1} \sum_m \langle a_{lm}^* a_{lm} \rangle$ . In Fig. 11 we show the Planck power spectra. We compare the frequency coadded foreground subtracted spectra on the left column and the single frequencies raw spectra on the right column. The comparison shows how the single frequency spectra exhibit some residuals on small angular scales. These residuals are given by the sum of different components which will be described in the following subsections.

### 4.2 Secondary anisotropies and foreground residuals in the likelihood

#### 4.2.1 Secondary anisotropies

**Thermal Sunyaev Zeldovich:** It is caused by the inverse Compton scattering of the CMB photons on high temperature electrons from the gas in galaxy clusters. The scattering produces a spectral distortion shifting photons towards higher energies by  $k_B T_e / m_e c^2$ , the signal has an analytic frequency dependence which in the non-relativistic limit is:  $f(x) = (x((e^x + 1)/(e^x - 1)) - 4)$  with  $x = (h\nu)/(k_B T_{CMB})$ . On the CMB angular power spectrum the Thermal SZ increases the power on small angular scales.

**Kinetic Sunyaev Zeldovich:** It is an additional effect given by a Doppler effect due to the peculiar motion of the cluster. The amplitude depends on the component along the line of sight of the cluster velocity. It is relevant for scales smaller than the ones observed by Planck for which the KSZ is a negligible effect, nevertheless it will be very important for future experiments.

**Lensing:** It is caused by the deflections of photons going through the Large Scale Structure during their path from the last scattering surface to the observer. The two main effects are a modification of the angular power spectrum in temperature where the lensing smooths the peaks and troughs, and the generation of B-mode polarization which dominates the small angular scales. It is investigated in the dedicated Planck paper [14].

#### 4.2.2 Foreground residuals

**Residual dust:** Dust is present up to the higher latitudes and therefore residual contributions must be considered at all scales even if using only a small patch of the sky like it is done in the high- $\ell$  likelihood.

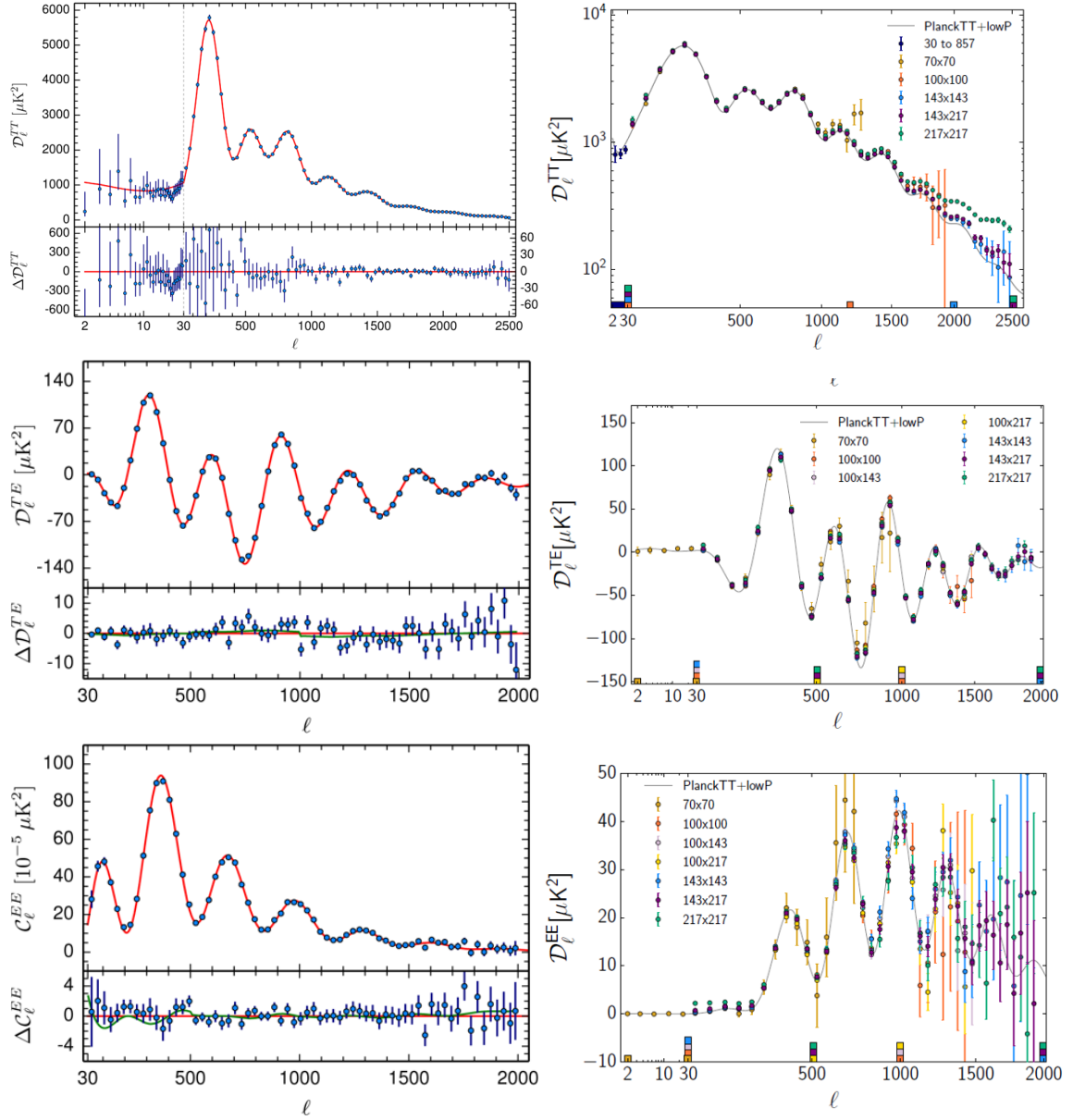


**Figure 11:** Planck angular power spectra. The first row is TT, the second row is the T-E cross correlation and the third row is the EE mode. The first column shows the frequency coadded foreground removed spectra, the second column the single frequencies raw spectra [13].

**Unresolved point sources:** Detected point sources are subtracted using dedicated masks but undetected sources still remains contaminating the signal at the smallest scales measured by Planck. In particular, one common contribution to all unresolved point sources is given by their simple random distribution in the sky, the so-called Poissonian term. It is a constant term given by the integration of the differential number counts up to the detection threshold flux. Infrared galaxies from the CIB have an additional contribution, the clustering term. The clustering of CIB is much more complex with respect to the Poissonian term and is modelled with a template based on the

measurements of the CIB done by Planck.

**CIBxTSZ:** The CIB and the TSZ cross correlate and this term must be properly accounted for in the likelihood.

All these signals are modelled within the likelihood with templates characterized by nuisance parameters which are varied inside the likelihood and are then marginalized over for the constraints on cosmological parameters. In Fig.12 we show the different templates for the secondary anisotropies and foreground residuals which have been used in the Planck likelihood.

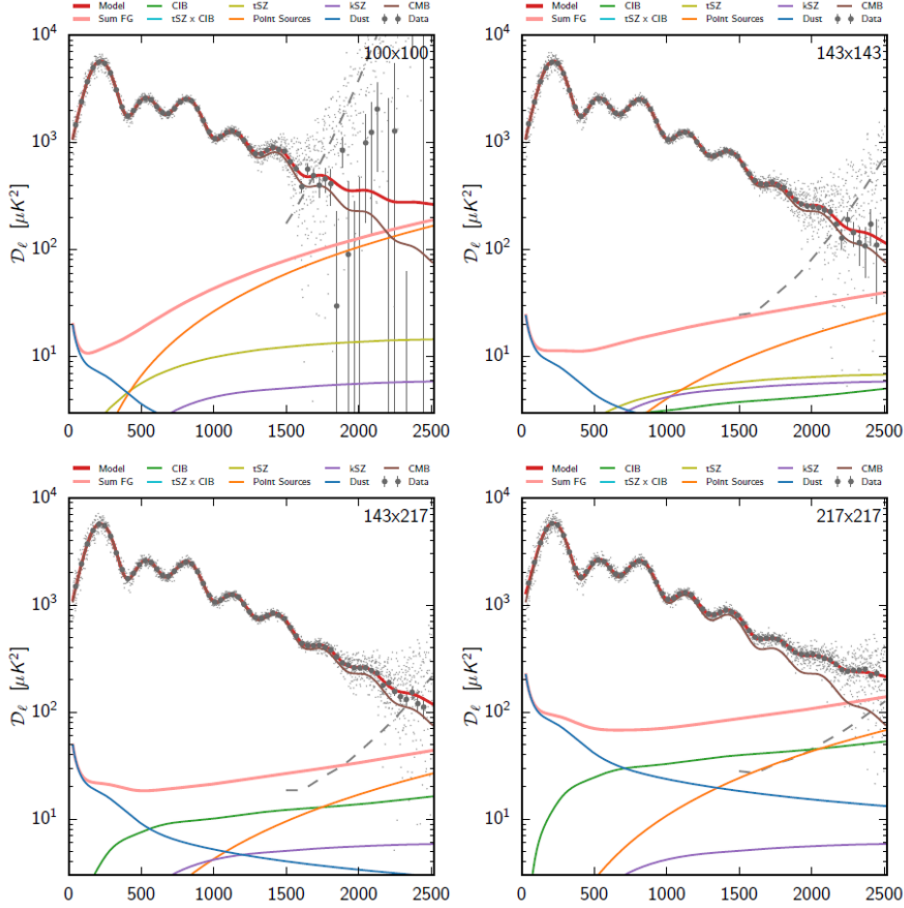


**Figure 12:** Foreground residuals and secondary anisotropies templates in the Planck likelihood [13].

### 4.3 An example: the case of primordial magnetic fields

The presence of secondary anisotropies and foreground residuals if not properly accounted for in the likelihood may bias the cosmological parameters derived from the data. The bias can lead to scientific interpretations which are not representative of the real underlying cosmological model but are simply a leakage of the effect of residuals not properly accounted for. One very significant example is the case of primordial magnetic fields. Magnetic fields on cosmological scales may be generated in the early Universe through different mechanisms and may provide the initial seeds which evolved into the magnetic fields we observe in the large scale structures like

in galaxies and clusters. If present before recombination magnetic fields leave different imprints on the CMB anisotropies (for a review see [15]). One of the imprints is an increase of the power on small angular scales which strongly resembles the contribution of unresolved point sources. In a pre-Planck case study [16] we considered the impact of small angular scale contamination by secondary anisotropies and foreground residuals on the constraints on primordial magnetic field amplitude. We considered the combination of data from WMAP and the South Pole Telescope. We compared the results with and without accounting for the residuals in the likelihood. We found that in the first case we obtained an upper limit on the amplitude of the fields as expected, in the case where the residuals were not considered in the likelihood instead we found a net detection of primordial magnetic fields of several nG. This detection is not the proof of existence of primordial magnetic fields but is due to the degeneracy of the residual contamination with the fields amplitude which biased the results. This test case demonstrates how it is crucial to account for the small angular scales contamination in the likelihood in order to not get a biased interpretation of the results.

## 5. The future is polarization

The Planck satellite has performed the definitive measurement of CMB anisotropies in temperature at the scales where the CMB is the dominant contribution in the microwave sky. Future experiments will be devoted to the observation of CMB polarization with the aim of performing a cosmic variance limited measurement as Planck did in temperature. But the CMB polarization is challenging not only from the instrumental point of view. In fact we have sources of contamination also in polarization which are by far lesser known than the temperature ones. On the small angular scales, point sources contribution is not very bright in polarization since only a fraction of sources is polarized. They did not represent an issue for Planck characteristics but may be relevant for future experiments [17]. The lensing of the large scale structure produces a B-mode signal on intermediate and small angular scales which cannot be removed but only reduced. The reduction is done with the de-lensing algorithm which are based on either CMB only data or cross correlations with the CIB or other astrophysical sources [18]. The methods are now in development in the perspective of future experiments with a target of 40% delensing capabilities.

On the large angular scales the dominant contribution at low frequency is the synchrotron emission which reaches up to the intermediate frequencies. Therefore to efficiently clean the CMB channels is necessary to have observations at the lowest frequencies to characterize the synchrotron emission. On higher frequencies the most important contamination especially for the B-mode polarization is thermal dust. Its contribution dominates the large angular scales but it affects also intermediate and smaller scales. It requires high frequency observations which are dominated by the dust contribution and may trace its behaviour. Since the high frequencies which are necessary cannot be observed from the ground experiments, and balloons cannot reach full sky coverage, the dust contamination is one of the reason why a space mission for CMB polarization is necessary to win the challenge of the primordial B-mode detection.

## 6. Conclusions

Planck represented and will represent a milestone for the knowledge of the microwave sky, with its nine frequency channels has performed full sky maps in temperature and polarization which are the status of the art of the microwave sky.

Cleaned CMB maps are at the basis of several analyses and some of the most important results achieved by Planck. The entire analysis dedicated to the study of the isotropy and the statistical properties of the CMB, which includes the search for anomalies, has been performed thanks to the production of CMB cleaned maps. It has confirmed the presence of large angular scales anomalies, although with not enough statistical significance, like the lack of power at the lowest multipoles, the point parity, the quadrupole and octupole alignment and the dipolar modulation. For more details we refer to the Planck 2015 dedicated paper [19]. The search for non-Gaussianities in the CMB anisotropies is also based on the CMB cleaned maps, the Planck precision allowed for the best measurement of the non-Gaussianity parameter in the three configurations  $f_{NL}^{Local} = 2.5 \pm 5.7$ ,  $f_{NL}^{equil} = -16 \pm 70$ ,  $f_{NL}^{ortho} = -34 \pm 33$  [20]. The lensing of the CMB by the large scale structure represents one of the most important results of Planck. It is a  $40 \sigma$  detection with the characterization of the lensing potential with unprecedented accuracy [14]. Moreover with the dedicated likelihood the lensing represents an independent Planck dataset which is used to derive cosmological results [14]. The lensing detection was possible thanks to the component separated maps and the four independent component separation methods used by Planck show perfect agreement. It was also possible to reconstruct a B-mode lensing all sky map using the lensing potential to predict the B-mode generated from the lensing of the measured E-mode and correlating this prediction with the measurement.

Planck has shown the complexity of the microwave sky changing the scenario of the astrophysical emissions showing unexpected dominant contributions in temperature and unprecedented precision measurements of polarized emissions. It has produced maps and derived the characteristics for all the diffuse foregrounds in temperature and polarization from the lowest to the highest frequencies providing the most accurate full sky model of microwave emissions to date.

The legacy of Planck not only represents the state of the art of full sky microwave observations, it has drawn the path to the future of CMB. The future of CMB observations is polarization but the foreground in polarization are still very poorly known and this requires a deep investigation. As long as foregrounds are not perfectly known beyond any doubt, any B-mode detection will not be fully reliable. Planck has been crucial in showing the importance of the knowledge of the microwave sky in polarization in B-mode studies, the inclusion of Planck 353 GHz data in the BICEP2 analysis has shown how important is the contamination by dust in the search of B-modes [12].

In order to characterize the single components the only possibility is to acquire data in the widest range of frequencies and in the highest number of channels. Only an high number of observational frequencies on a wide range can provide sufficient data to characterize the sky model with a sufficient accuracy. The lensing represents a further challenge. On small angular scales B-modes signal are dominated by the lensing and the only possibility to observe a cosmological signal are delensing algorithms which need high resolution to perform at best. This means that the future is not only a question of frequencies and sensitivity but also of high resolution optics. In Fig. 13 we

show the status of observations and the prediction of the foreground emissions in polarization.

Planck 2018 release was delivered after this talk was discussed [4], it confirmed the results of the previous release improving in the characterization of microwave astrophysical emissions especially on the high frequencies and improving the cosmological results with the improvement of the polarization on large and small angular scales. Planck results represent the current status of CMB cosmology and Planck data will represent the stress test of all possible cosmological models which will be discussed in the future. Its legacy on the microwave sky has shown how it is complex in both temperature and polarization and has prepared the ground for future experiments.

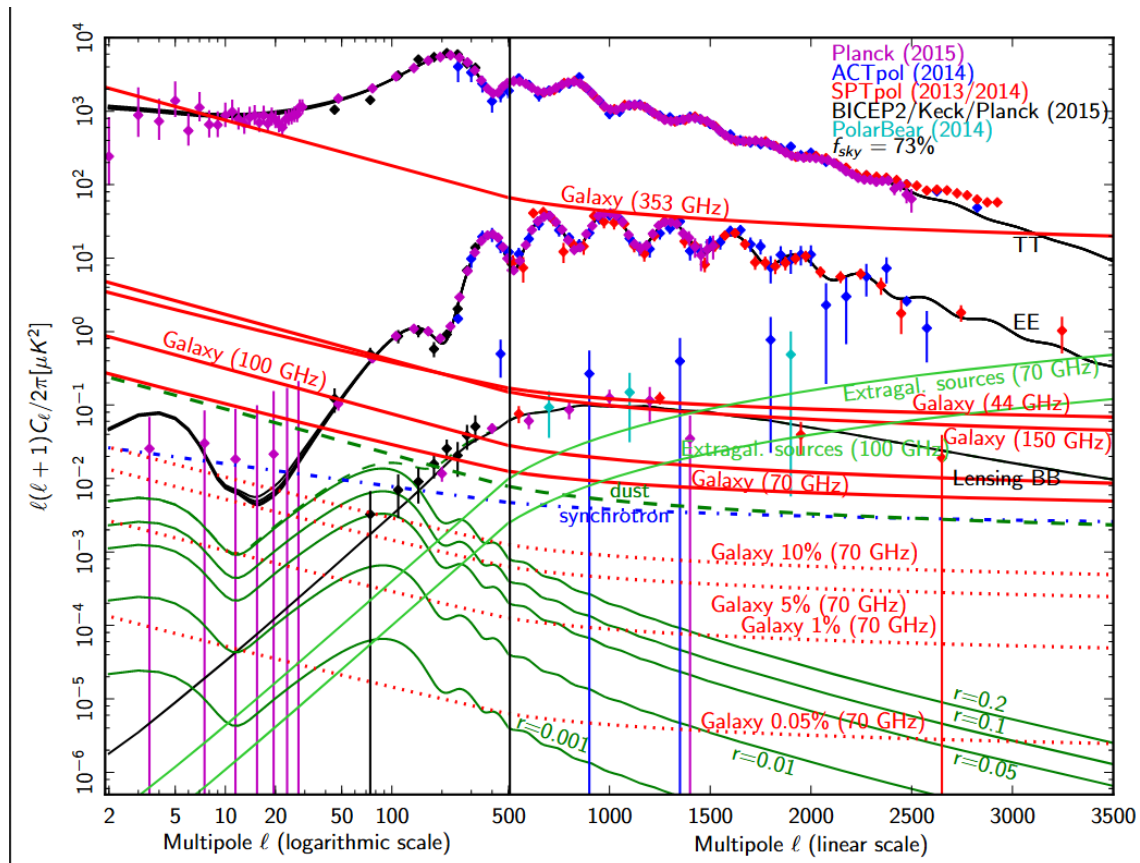


**Figure 13:** CMB anisotropies theoretical spectra and data with the prediction for the foreground contamination on large angular scales.

## References

- [1] D. J. Fixsen, “The Temperature of the Cosmic Microwave Background,” *Astrophys. J.* **707** (2009) 916 doi:10.1088/0004-637X/707/2/916 [arXiv:0911.1955 [astro-ph.CO]].
- [2] Planck Collaboration, “Planck 2015 results. I. Overview of products and scientific results,” *Astron. Astrophys.* **594** (2016) A1 doi:10.1051/0004-6361/201527101 [arXiv:1502.01582 [astro-ph.CO]].
- [3] Planck Collaboration, “Planck 2013 results. I. Overview of products and scientific results,” *Astron. Astrophys.* **571** (2014) A1 doi:10.1051/0004-6361/201321529 [arXiv:1303.5062 [astro-ph.CO]].

- [4] Planck Collaboration, “Planck 2018 results. I. Overview and the cosmological legacy of Planck,” arXiv:1807.06205 [astro-ph.CO].
- [5] H. K. Eriksen *et al.*, “Power spectrum estimation from high-resolution maps by Gibbs sampling,” *Astrophys. J. Suppl.* **155** (2004) 227 doi:10.1086/425219 [astro-ph/0407028].
- [6] H. K. Eriksen, J. B. Jewell, C. Dickinson, A. J. Banday, K. M. Gorski and C. R. Lawrence, “Joint Bayesian component separation and CMB power spectrum estimation,” *Astrophys. J.* **676** (2008) 10 doi:10.1086/525277 [arXiv:0709.1058 [astro-ph]].
- [7] C. L. Bennett *et al.* [WMAP Collaboration], “Nine-Year Wilkinson Microwave Anisotropy Probe (WMAP) Observations: Final Maps and Results,” *Astrophys. J. Suppl.* **208** (2013) 20 doi:10.1088/0067-0049/208/2/20 [arXiv:1212.5225 [astro-ph.CO]].
- [8] Haslam, C. G. T., Klein, U., Salter, C. J., et al. 1981, *Astron. Astrophys.* **100**, 209
- [9] Planck Collaboration, “Planck 2015 results. IX. Diffuse component separation: CMB maps,” *Astron. Astrophys.* **594** (2016) A9 doi:10.1051/0004-6361/201525936 [arXiv:1502.05956 [astro-ph.CO]].
- [10] Planck Collaboration, “Planck 2015 results. X. Diffuse component separation: Foreground maps,” *Astron. Astrophys.* **594** (2016) A10 doi:10.1051/0004-6361/201525967 [arXiv:1502.01588 [astro-ph.CO]].
- [11] Planck Collaboration, “Planck 2015 results. XXV. Diffuse low-frequency Galactic foregrounds,” *Astron. Astrophys.* **594** (2016) A25 doi:10.1051/0004-6361/201526803 [arXiv:1506.06660 [astro-ph.GA]].
- [12] BICEP2 and Planck Collaborations, *Phys. Rev. Lett.* **114** (2015) 101301 doi:10.1103/PhysRevLett.114.101301 [arXiv:1502.00612 [astro-ph.CO]].
- [13] Planck Collaboration, “Planck 2015 results. XI. CMB power spectra, likelihoods, and robustness of parameters,” *Astron. Astrophys.* **594** (2016) A11 doi:10.1051/0004-6361/201526926 [arXiv:1507.02704 [astro-ph.CO]].
- [14] Planck Collaboration, “Planck 2015 results. XV. Gravitational lensing,” *Astron. Astrophys.* **594** (2016) A15 doi:10.1051/0004-6361/201525941 [arXiv:1502.01591 [astro-ph.CO]].
- [15] Planck Collaboration, “Planck 2015 results. XIX. Constraints on primordial magnetic fields,” *Astron. Astrophys.* **594** (2016) A19 doi:10.1051/0004-6361/201525821 [arXiv:1502.01594 [astro-ph.CO]].
- [16] D. Paoletti and F. Finelli, “Constraints on a Stochastic Background of Primordial Magnetic Fields with WMAP and South Pole Telescope data,” *Phys. Lett. B* **726** (2013) 45 doi:10.1016/j.physletb.2013.08.065 [arXiv:1208.2625 [astro-ph.CO]].
- [17] G. Puglisi *et al.*, “Forecasting the Contribution of Polarized Extragalactic Radio Sources in CMB Observations,” *Astrophys. J.* **858** (2018) no.2, 85. doi:10.3847/1538-4357/aab3c7
- [18] J. Errard, S. M. Feeney, H. V. Peiris and A. H. Jaffe, “Robust forecasts on fundamental physics from the foreground-obscured, gravitationally-lensed CMB polarization,” *JCAP* **1603** (2016) no.03, 052 doi:10.1088/1475-7516/2016/03/052 [arXiv:1509.06770 [astro-ph.CO]].
- [19] Planck Collaboration, “Planck 2015 results. XVI. Isotropy and statistics of the CMB,” *Astron. Astrophys.* **594** (2016) A16 doi:10.1051/0004-6361/201526681 [arXiv:1506.07135 [astro-ph.CO]].
- [20] Planck Collaboration, “Planck 2015 results. XVII. Constraints on primordial non-Gaussianity,” *Astron. Astrophys.* **594** (2016) A17 doi:10.1051/0004-6361/201525836 [arXiv:1502.01592 [astro-ph.CO]].

## **DISCUSSION**

**DMTRI WIEBE:** There is the so called Goldreich-Kylafis effect that may cause CO line emission to be polarized. Can it somehow interfere with the future CMB experiments?

**DANIELA PAOLETTI:** Within Planck the residual CO emission is quite relevant even after component separation, since it contributes to the temperature to polarization leakage the CO emission regions are masked with a dedicated mask in the polarization analysis preventing it to also contribute directly in polarization.